Available online at www.sciencedirect.com
SCIENCE DIRECT®
Chemical Physics Letters 404 (2005) 90–94
CHEMICAL PHYSICS LETTERS
www.elsevier.com/locate/cplett

Deuterium 3D NMR experiments for analysing weakly aligned, isotopically enriched solutes

Olivier Lafon, Philippe Lesot *

Laboratoire de Chimie Structurale Organique, CNRS UMR 8074, ICMMO, Bât. 410, Université de Paris-Sud XI, Institut de Chimie Moléculaire et des Matériaux d'Orsay, UMR 8074, 91405 Orsay Cedex, France

Received 20 December 2004; in final form 11 January 2005

Abstract

In this contribution we report three new pure absorption mode deuterium 3D NMR experiments to analyse spectra of isotopically enriched solutes dissolved in weakly orienting liquid crystals. The potentialities of these 3D strategies are illustrated using the perdeuterated 1-butanol, a prochiral molecule of C_s symmetry in average, dissolved in a chiral mesophase made of poly-γ-benzyl-L-glutamate. The experimental results obtained for the three types of experiments are discussed and compared.

1. Introduction

Deuterium NMR is a well-established spectroscopic method for examining microscopic properties (C–D order parameters, dynamics properties, molecular geometry,...) of isotopically enriched mesogenic molecules in the nematic phase or oriented solutes [1,2].

In the case of weakly aligned deuterated solutes, the magnitude of quadrupolar splittings does not generally exceed the dispersion of ^{2}H chemical shifts, so ^{2}H 1D NMR spectra with non-symmetrical aspect are observed [1]. Consequently, for large size enriched molecules, the ^{2}H spectra can become complex to analyse (peak overlaps) and require the use of multidimensional NMR. This situation is more exacerbated when studying chiral or prochiral molecules oriented in chiral liquid-crystalline phases due to the spectral discrimination between enantiomers or enantiotopic directions [2–5].

Different autocorrelation 2D pulse sequences, such as δ-resolved, Q-resolved, Q-COSY or Q-DQ [6,7] and more recently, the Q-resolved Fz and Q-COSY Fz sequences [8] have been proposed for correlating the two components of a deuterium quadrupolar doublet. To the best of our knowledge, the use of ^{2}H homonuclear 3D experiments was never explored so far, and therefore merited some particular attention considering the variety of applications using aligned isotopically enriched molecules. In this preliminary work, three types of 3D sequences were explored and are reported. Their efficiency was experimentally illustrated using the perdeuterated 1-butanol dissolved in an organic solution of poly-γ-benzyl-L-glutamate (PBLG) [3].

2. Theoretical analysis

The common idea associated with 3D experiments described here is to obtain 3D ^{2}H spectra where the acquisition dimension (F_3) contains simultaneously ^{2}H chemical shifts, δ, and quadrupolar splittings, $\Delta\nu_Q$, while the other dimensions (F_2 and F_1) show separately these data. In this aim, three pulse schemes with different coherence pathways are possible as seen in Fig. 1. The major difference between them originates from the coherence orders excited during the second evolution

* Corresponding author. Fax: +33 1 69 15 81 05.
E-mail address: philesot@icmo.u-psud.fr (P. Lesot).

0009-2614/$ - see front matter © 2005 Elsevier B.V. All rights reserved.
doi:10.1016/j.cplett.2005.01.040

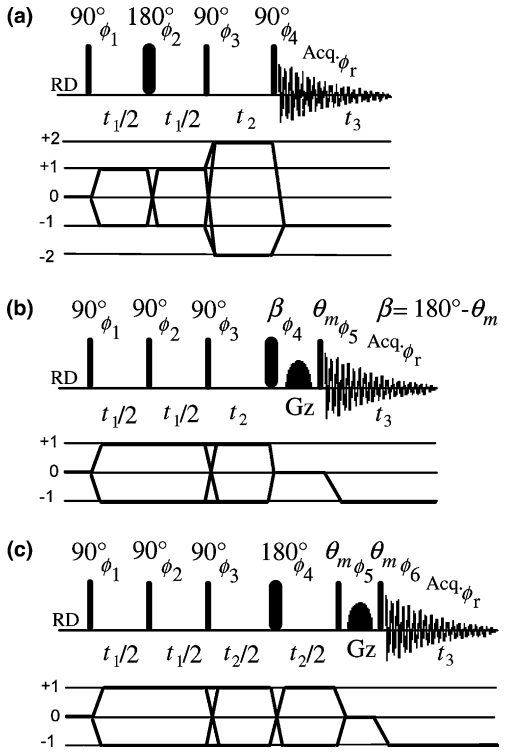

Fig. 1. Pulse scheme and coherence pathway diagrams of 3D sequences: (a) *Q*-DQ 3D experiment using $\phi_1 = \phi_2 = 16(x)$; $\phi_3 = 4(x), 4(-x), 4(y), 4(-y)$; $\phi_4 = 4(x, y, -x-y)$, $\phi_r = -x, y, x, -y, y, x, -y, -x, x, -y, -x, y, -y, -x, y, x$; (b) δ-resolved/Q-COSY 3D experiment using $\phi_1 = 8(x), 8(-x)$; $\phi_2 = 4(x, y, -x, -y)$; $\phi_3 = 4(x), 4(-x), 4(x), 4(-x)$; $\phi_4 = \phi_5 = 16(x)$; $\phi_r = 8(x), 8(-x)$; (c) pulse scheme of the δ, *Q*-resolved 3D experiment using $\phi_1 = 8(x), 8(-x)$; $\phi_2 = 4(x, y, -x, -y)$; $\phi_3 = 4(x)$, $4(-x)$, $4(x)$, $4(-x)$; $\phi_4 = \phi_5 = \phi_6 = 16(x)$; $\phi_r = 8(x)$, $8(-x)$. For (b)–(c) sequences $\theta_m = 54.7°$. A 180° composite pulse can be applied to reduce offset effects and non-ideal flip angles [9].

period (t_2) of the 3D sequence. The main characteristics of the three 3D experiments examined here are listed in Table 1.

2.1. The Q-DQ 3D experiment

This sequence, shown in Fig. 1a, is a '3D version' of the *Q*-DQ 2D experiment in which the fixed refocusing delay τ is now replaced by a variable time period [6]. This solution optimizes the condition for transferring the ^{2}H single quantum coherences (SQCs) into double quantum coherences (DQCs) that evolve during t_2 [10]. As a direct consequence, the difficult choice of the τ value when the range of $\Delta\nu_Q$s is wide, is now removed. Selection of DQCs is efficiently performed by a four-step phase cycling, while their conversion into an observable ^{2}H signal is performed by the last 90° pulse [11]. Using the spin-1 operator product formalism [7], the signal equation in the three dimensions were calculated for a single deuteron. After a four-step phase cycle and disregarding all relaxation and phase terms, the expression of the signal is:

$$S(t_1, t_2, t_3) \propto 4\sin[\omega_Q t_1] \times \cos[2\omega_D t_2] \times \left(\sin[\omega_Q t_3] e^{i[(\omega_D) t_3]}\right), \quad (1)$$

with $\omega_D = 2\pi\nu_D$ and $\omega_Q = \pi\Delta\nu_Q$. As expected, the ^{2}H chemical shifts (centre of the quadrupolar doublets) evolve during t_2 at the double of the frequencies compared with 1D spectra, thus showing the DQ character of coherences.

During the t_2 variable period, the quadrature is performed using a States or TPPI sampling scheme, combined with 45° phase increments for the three first pulses. In contrast, the signal during the first evolution period t_1 has a sine-modulated component ($\sin[\omega_Q t_1]$), and hence the QSEQ sampling scheme can be applied in this dimension. After a triple Fourier transform (FT), pure absorption resonances are obtained.

2.2. The δ-resolved/Q-COSY 3D experiment

The second 3D pulse scheme explored is shown in Fig. 1b. It derives from the combination of the δ-resolved and *Q*-COSY 2D experiments developed recently [6]. As it can be seen in the transfer coherence pathway diagram, this experiment differs from the *Q*-DQ 3D experiment as only ±1 quantum coherence orders are involved throughout the pulse sequence. This strategy can be seen as an advantage because the one quantum deu-

Table 1
Comparative table of three 3D autocorrelation deuterium NMR experiments proposed

Experiment features	3D *Q*-DQ	3D δ-resolved/*Q*-COSY	3D δ, Q-resolved
Coherence order during t_2	±2	±1	±1
Pulse number	4	5	6
z-gradient filter	n	y	y
Minimum number of phase cycle steps	4	8	8
Data sampling scheme in t_1	QSEQ	States/TPPI	States/TPPI
Data sampling scheme in t_2	States/TPPI	States/TPPI	States/TPPI
Spectral information in F_1 dimension	$\Delta\nu_Q$	δ	δ
Spectral information in F_2 dimension	2δ	$\delta, \Delta\nu_Q$	$\Delta\nu_Q$
Relative *S*/*N* ratio[a]	1	1/3	1/3

[a] *S*/*N* ratio is evaluated for an equivalent number of acquisitions (eight scans) and after the FT. The relative *S*/*N* ratio of the *Q*-DQ 3D experiment is used as reference and is equal to one.

terium signal evolving during t_2 is much less sensitive to B_o magnetic field inhomogeneities and pulse imperfections [10]. The selection of the desired coherence pathways is achieved by this phase cycling. After an eight-step phase cycle and disregarding all relaxation terms phase, the signal expression is:

$$S(t_1,t_2,t_3) \propto \tfrac{4}{3}\sin[\omega_D t_1] \times \begin{pmatrix} \sin[(\omega_D-\omega_Q)t_2]e^{i[(\omega_D+\omega_Q)t_3]} \\ -\sin[(\omega_D+\omega_Q)t_2]e^{i[(\omega_D-\omega_Q)t_3]} \end{pmatrix}. \quad (2)$$

The above equation shows that only ^{2}H frequencies associated with SQCs are generated throughout the pulse sequence. To record the 3D experiment with pure absorption mode, we used a z-gradient filter with appropriate pulse angles and phases. This solution was recently adopted for recording Q-resolved and Q-COSY 2D spectra with pure absorption mode [8]. States or TPPI sampling scheme can be used to generate the quadrature detection in F_1 and F_2 dimensions.

2.3. The 3D δ, Q-resolved experiment

As previously, the third and last deuterium 3D sequence developed involves SQCs during the t_2 evolution period (see diagram in Fig. 1c). This 3D experiment is a variant of the previous ones that combines the δ-resolved and Q-resolved Fz experiments. Here, again an eight-step phase cycling is necessary to remove the undesired coherence transfer pathways. After a complete phase cycling and disregarding all relaxation and phase terms, the signal expression is:

$$S(t_1,t_2,t_3) \propto \tfrac{4}{3}\sin[\omega_D t_1]\sin[\omega_Q t_2] \times \left(e^{i[(\omega_D-\omega_Q)t_3]} - e^{i[(\omega_D+\omega_Q)t_3]}\right). \quad (3)$$

As expected, this equation shows that only ^{2}H frequencies associated with SQCs are generated by the sequence. States or TPPI sampling scheme can be applied to provide quadrature detection in F_1 and F_2 dimensions. The main difference between this 3D experiment and the previous one lies in the refocusing of chemical shifts during the t_2 period. Thus, in this last case, we totally separate chemical shift and quadrupolar information.

2.4. Relative sensitivity

In 3D experiments, the sensitivity is major a problem. Table 1 reports the relative S/N ratio calculated for the same number of scans and after three FT. From the signal expressions, we can show that the δ-resolved/Q-COSY and the δ, Q-resolved 3D experiments have the same sensitivity with a reduction by a factor of 3 compared with the Q-DQ 3D experiments. This loss of sensitivity results both from the z-gradient filter used for obtaining pure absorption mode resonances [8] and the echo sequence used for refocussing the quadrupolar interaction during t_1 [12]. Actually for prevailing the refocussing of ^{2}H chemical shifts, the coherence order before and after the second 90° pulse must be the same ($\Delta p = 0$) (Fig. 1b and c). For this, a four-step phase cycling is required, but this procedure removes half of the coherence transfer pathways. Hence, a choice between sensitivity and resolution must be unfortunately done.

3. Experimental

The sample of perdeuterated 1-butanol (**1**) in PBLG was prepared using 100 mg of polymer (DP = 1132, MW ≈ 248 000), 15 mg of solute, and 360 mg of chloroform. Other details on the sample preparation can be found in [3]. All experiments were carried out at 302 K using a Bruker DRX 400 spectrometer equipped with a direct 5 mm broadband probe (61.4 MHz for deuterium). The 90° ^{2}H pulse was 9.5 μs and a sinus shape gradient pulse (24 G/cm along z) with length of 2 ms was used [7]. Protons was decoupled using WALTZ-16 sequence in order to remove possible residual ^{2}H–^{1}H couplings (enrichment < 100%). All 3D spectra were recorded with 16 scans per FID and $80 \times 90 \times 384$ data points in t_1, t_2, t_3 dimensions, respectively. The recycling time was set to 0.4 s to reduce the total experimental time to 14 h. All 3D matrices were processed to a resolution of $128(F_1) \times 128(F_2) \times 512(F_3)$ data points prior to the triple FT and a Lorentzian filtering was applied in the three dimensions. Neither linear prediction nor maximum entropy process were performed to reconstruct the NMR signal [10].

4. Results and discussion

To illustrate the utility of the 3D NMR experiments described above, we investigated the case of isotopically enriched 1-butanol in the PBLG/$CHCl_3$ mesophase. This flexible prochiral molecule of C_s symmetry in average possesses C–D enantiotopic directions in each methylene group that are in principle discriminated in a chiral oriented solvent [5]. Consequently, we may a priori observe a maximum number of seven quadrupolar doublets corresponding to the various different inequivalent deuterons including enantiotopic directions but disregarding the hydroxyl group. The ^{2}H–{^{1}H} spectrum of **1** displayed in Fig. 2 shows typically a non-symmetrical aspect due to the magnitude of the quadrupolar splittings (from 42 to 396 Hz) compared with the largest difference of chemical shift (160 Hz). Due to the weak alignment of solutes in PBLG, the ^{2}H–^{2}H total couplings (scalar and dipolar) are generally included in the linewidths of doublet components, and so no further

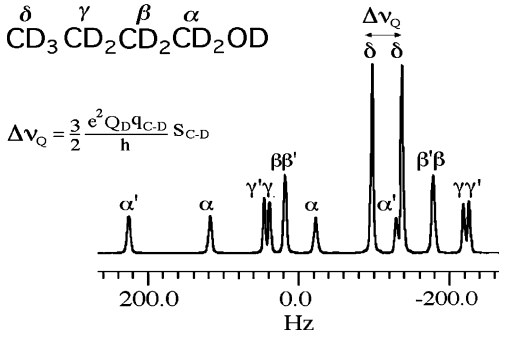

Fig. 2. ^{2}H 1D (61.4 MHz) spectrum of **1** recorded with 2048 data points and 64 scans. No filtering is applied. In the equation displayed, Q_D is the ^{2}H nuclear quadrupole moment, q_{C-D} is the electric field gradient along the C–D bond and S_{C-D} is the order parameter of the C–D direction ($-0.5 \leqslant S_{C-D} \leqslant 1$). The assignment of the doublets is based on the analysis of the 3D spectra reported below.

spectral patterns are visible. In this spectrum we observe twelve resonances that should be assigned to seven non-equivalent deuterium sites (disregarding the OD group).

In Fig. 3, we display the *Q*-DQD 3D spectrum of **1** and the three associated 2D positive projections. As expected all peaks can be phased in pure absorption mode. When plotting both positive and negative levels, the 'data cube' shows simultaneously 24 peaks, half of them showing a positive phase. This is a consequence of the sine-modulation of quadrupolar splittings during the t_1 and t_3 periods (see Eq. (1)), thus leading to an antiphase character of doublets in F_1 and F_3 dimensions. Note that all relevant information can be extracted from the analysis of signals with positive or negative phase. The F_2/F_3 plane is similar the *Q*-DQ 2D spectrum, but in this case the intensity of resonances associated with DQ coherences is maximum whatever the magnitude of the quadrupolar splittings. The 2D plot corresponding to the F_2/F_3 plane is formally equivalent to a δ-resolved map except that resonance frequencies associated with each non-equivalent ^{2}H nuclei in F_2 are doubled, thus increasing the dispersion of δs by a factor of two. The simultaneous analysis of the 3D spectrum allow to correlate simply the two components of each doublet, and then assign them on the basis of chemical shifts (see Fig. 3b–d). Thus the most deshielded and shielded pairs of doublets corresponds to the α-methylene and the methyl group, respectively. Note that the pro-*R* and pro-*S* deuterons in the α- and γ-methylene groups are discriminated but no spectral enantiodiscrimination is detected for the β-methylene group [5]. In this example, the enantiotopic discrimination for the two deuterons on the methylene group attached to the hydroxyl group is relatively large (216 Hz).

In Fig. 4, the δ-resolved/*Q*-COSY 3D spectrum of **1** and the corresponding 2D projections are shown. As expected all peaks can be phased in pure absorption mode, but in this case only 12 in-phase peaks are detected. The reduction of number of autocorrelation peaks increases substantially the legibility of 3D spectrum compared with the *Q*-DQD 3D spectrum. 2D contour plot associated with the F_2/F_3 plane is formally equivalent to a *Q*-COSY 2D spectrum where the ^{2}H doublets are distributed along the diagonal. The 90° pulse in the midpoint of the t_1 period serves to refocus the quadrupolar interaction, and hence only δs appear in F_1 dimension after the third FT. This situation is attractive because the rather small dispersion of ^{2}H chemical shifts (≈10 ppm) requires less data points in this dimension. From the analytical point of view, the assignment of doublets is identical to the previous one.

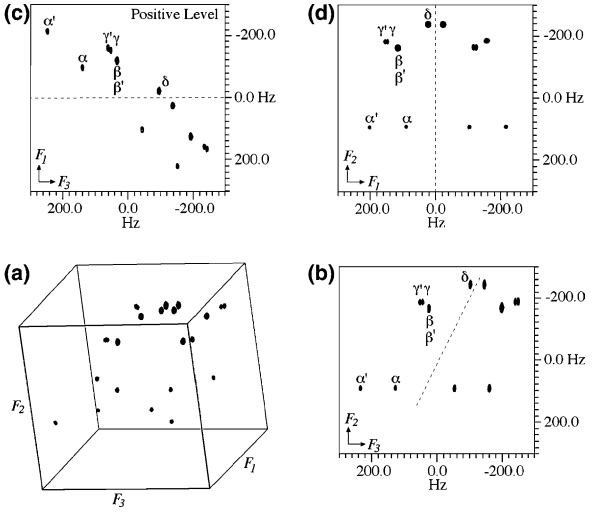

Fig. 3. (a) *Q*-DQ 3D spectrum of **1**. (b–d) 2D maps associated with the F_2/F_3, F_1/F_3 and F_2/F_1 positive projections. Information for each plane is $(2\delta/\delta, \Delta\nu_Q)$, $(\Delta\nu_Q/\delta, \Delta\nu_Q)$ and $(2\delta/\Delta\nu_Q)$, respectively. Dashed lines show the middle of each doublet.

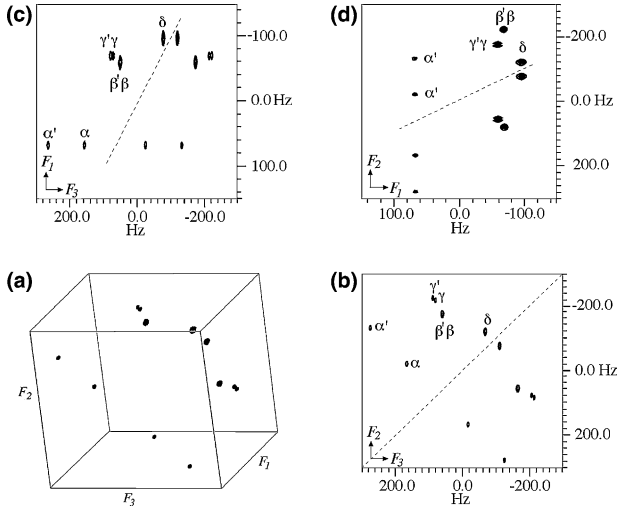

Fig. 4. (a) δ-resolved/*Q*-COSY 3D spectrum of **1**. (b–d) 2D maps associated with the F_2/F_3, F_1/F_3 and F_2/F_1 projections. Information for each plane is $(\delta, \Delta\nu_Q/\delta, \Delta\nu_Q)$, $(\delta/\delta, \Delta\nu_Q)$ and $(\delta, \Delta\nu_Q/\delta)$, respectively.

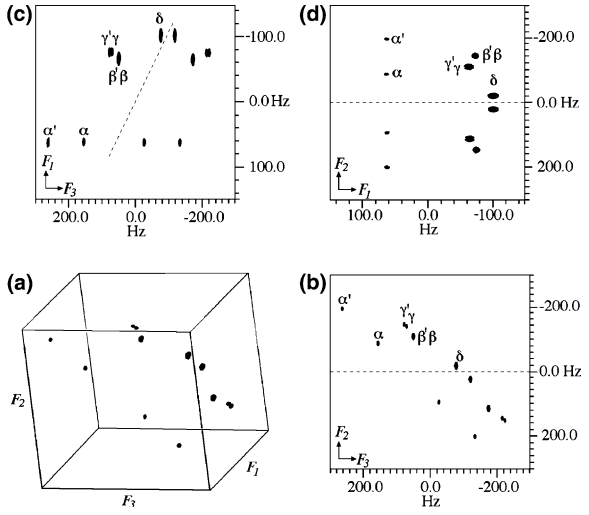

Fig. 5. (a) δ, Q-resolved 3D spectrum of **1**. (b–d) 2D maps associated with the F_2/F_3, F_1/F_3 and F_2/F_1 projections. Information for each plane is $(\Delta\nu_Q/\delta, \Delta\nu_Q)$, $(\delta/\delta, \Delta\nu_Q)$ and $(\Delta\nu_Q/\delta)$, respectively.

Finally, Fig. 5 presents the δ, Q-resolved 3D spectrum of **1**. This last experiment can be seen as a variant of the δ-resolved/Q-COSY 3D experiment in which δs are refocused during the t_2 period. As a consequence the 2D contour plots associated with the F_1/F_3 and F_2/F_3 planes are formally equivalent to the δ-resolved and Q-resolved maps. The third plane, F_1/F_2, provides an interesting 2D spectrum where δs are eliminated in F_2 while $\Delta\nu_Q$s are cancelled in the F_1 dimension. In this plane we totally separate two relevant information as in the case of the tilted Q-resolved 2D maps, but with no tilt procedure. This situation would not be easily performed with a 2D experiment, because it requires the refocusing of quadrupolar interaction during the acquisition, by inserting a deuterium 90° hard pulse in the middle of each dwell time [10]. The δ, Q-resolved 3D experiment offers an elegant alternative to this unusual acquisition scheme.

5. Conclusions

In our quest of new NMR tools for analysing weakly aligned perdeuterated solutes, we propose the use of 3D experiments to facilitate the assignment of quadrupolar doublets in overcrowded ^{2}H 1D spectra. All 3D sequences described here lead to pure absorption mode peaks and as they contain few rf-pulses, only a small amount of magnetization is lost due to pulse imperfections, i.e. inaccurate flip angles or B_1 inhomogeneities. These 3D sequences differ from each other by the spectral information displayed in the three spectral dimensions. Using this approach, it becomes now possible to totally separate ^{2}H chemical shift and quadrupolar interaction without post-acquisition treatment (tilt). In addition the reduction of spectral widths produced by the separation of δs and $\Delta\nu_Q$s leads to better digitalization resolution for the same acquisition time.

Acknowledgements

The authors acknowledge Profs B. Ancian and J. Courtieu for their helpful discussions.

References

[1] R.Y. Dong, Annu. Rep. NMR Spectrosc. 53 (2004) 68.
[2] J.W. Emsley, P. Lesot, D. Merlet, Phys. Chem. Chem. Phys. 6 (2004) 522.
[3] M. Sarfati, P. Lesot, D. Merlet, J. Courtieu, Chem. Commun. (2000) 2069, and references therein.
[4] P. Lesot, M. Sarfati, J. Courtieu, Chem. Eur. J. 9 (2003) 1724.
[5] C. Aroulanda, D. Merlet, J. Courtieu, P. Lesot, J. Am. Chem. Soc. 123 (2001) 12059.
[6] D. Merlet, B. Ancian, J. Courtieu, P. Lesot, J. Am. Chem. Soc. 121 (1999) 5249.
[7] D. Merlet, M. Sarfati, B. Ancian, J. Courtieu, P. Lesot, Phys. Chem. Chem. Phys. J. 2 (2000) 2283.
[8] O. Lafon, P. Lesot, D. Merlet, J. Courtieu, J. Magn. Reson. 171 (2004) 134.
[9] M.H. Levitt, NMR Encyclopedia, Wiley, Chichester, 1996, p. 1396.
[10] R.R. Ernst, G. Bodenhausen, A. Wokaun (Eds.), Principles of Nuclear Magnetic Resonance in One and Two Dimensions, Clarendon Press, Oxford, 1987.
[11] M.H. Levitt, Spin Dynamics, Wiley, Chichester, 2001.
[12] S. Antonijevic, S. Wimperis, J. Magn. Reson. 164 (2003) 343.